Original Article
THZ1, a covalent CDK7 inhibitor, enhances gemcitabine-induced cytotoxicity via suppression of Bcl-2 in urothelial carcinoma

Kuan-Lin Kuo[1,2*], Wei-Chou Lin[3*], Shing-Hwa Liu[1], Fu-Shun Hsu[4,5], Yu Kuo[6], Shih-Ming Liao[2], Shao-Ping Yang[2], Zuo-He Wang[2], Chen-Hsun Hsu[2], Kuo-How Huang[2]

[1]Graduate Institute of Toxicology, College of Medicine, National Taiwan University, Taipei, Taiwan; [2]Department of Urology, College of Medicine, National Taiwan University and National Taiwan University Hospital, Taipei, Taiwan; [3]Department of Pathology, National Taiwan University Hospital, Taipei, Taiwan; [4]Department of Urology, Yang Ming Branch of Taipei City Hospital, Taipei, Taiwan; [5]Graduate Institute of Clinical Medicine, College of Medicine, National Taiwan University, Taipei, Taiwan; [6]Department of Radiology and Nuclear Medicine, Taipei Veterans General Hospital, Taipei, Taiwan. *Equal contributors.

Abstract: Chemotherapy with gemcitabine plus cisplatin remains the mainstay of treatment for metastatic urothelial carcinoma (UC); however, drug resistance occurs in most patients and eventually leads to treatment failure. In this study, we investigated the role of cyclin-dependent kinase 7 (CDK7) regulation in the treatment of human UCs. Moreover, we studied the effect of THZ1, a CDK7 inhibitor, alone and in combination with gemcitabine, on UCs and explored the underlying mechanism. Immunohistochemical staining showed that CDK7 expression was significantly higher in UC tumors than in counterpart urothelium. THZ1 elicited dose-dependent cytotoxicity and apoptosis in two high-grade UC cells (BFTC905 and T24). THZ1 co-treatment potentiated gemcitabine-induced cytotoxicity with suppression of B-cell lymphoma 2 (Bcl-2). Studies with a xenograft nude mouse model also confirmed that THZ1 enhanced the antitumor effect of gemcitabine on UC. These findings provide important pilot data to target CDK7 or Bcl-2 for the treatment of UCs and for overcoming chemoresistance in UCs.

Keywords: Urothelial carcinoma, CDK7, Bcl-2, gemcitabine, THZ1

Introduction

Urothelial carcinoma (UC) was the sixth most prevalent cancer and accounted for nearly 74,000 new cases of cancer within the United States in 2015 [1]. Nearly 50% of the cases with muscle-invasive UCs show metastasis even after radical cystectomy. Systemic chemotherapy remains the mainstay of treatment for metastatic UC [2]. Gemcitabine in combination with cisplatin (GC) is the current standard of care for first-line treatment in suitable patients. Nevertheless, the response rate and 5-year survival rate of chemotherapy in such patients have been found to be approximately 50% and 20%, respectively [3, 4]. Drug resistance exists or occurs inevitably, which causes relapse and ominous outcomes. Thus, it is imperative to find novel strategies to improve chemotherapy sensitivity or circumvent chemotherapy resistance.

Currently, cisplatin (cis-diamminedichloroplatinum II, CDDP) is the main component of chemotherapy for metastatic UCs. The antitumor mechanism of cisplatin involves crosslinking with purine DNA bases and forming DNA adducts to hinder DNA replication and transcription [2]. Gemcitabine, a nucleotide analog, replaces cytidine during DNA replication and blocks new DNA formation, thus causing cell death. Several genetic and epigenetic pathways have been reported to contribute to drug resistance [3, 4]. Altered expression patterns of anti-apoptotic and pro-apoptotic proteins have been linked to decreased apoptosis [5-7]. Downregulated B-cell lymphoma-2 (Bcl-2) family pro-apoptotic proteins have been well explored in

this aspect [4, 8-10] and drug resistance to gemcitabine has been linked to increased expression of anti-apoptotic Bcl-2 in several solid tumors.

Cyclin-dependent kinases (CDKs/cyclins) play an essential role in regulating major biological functions such as cell differentiation, growth, proliferation, metabolism, and cell cycle progression [5]. RNA polymerase II (RNAPII)-catalyzed gene transcription is a critical process facilitated by multiple transcription factors [4, 5]. During transcription initiation and elongation, CDK7 phosphorylates the RNAPII C-terminal domain at serines 5 and 7 to participate in the initiation and elongation of transcription [8]. Dysregulated CDK activity is associated with various cancers [6]. Targeting CDK regulation is emerging as a promising anticancer therapy [6, 7]; however, some CDK inhibitors elicit non-selective CDK inhibition and off-target kinase interactions, which detrimentally affect normal cells and induce intolerable adverse effects [8-10]. THZ1 is a selective inhibitor of CDK7. Although THZ1 inhibits the CDK7-mediated transcriptional process and suppresses tumor growth in several human tumors, its antitumor effect has not been studied in UCs [11-13].

In this study, we investigated the therapeutic efficacy of THZ1 alone and in combination with gemcitabine or cisplatin in human UC *in vitro* and *in vivo*. Furthermore, we explored the antitumor mechanism of the drug combination, involving anti-apoptotic Bcl-2 regulation.

Materials and methods

Cell culture

The Taiwan Bioresource Collection and Research Center was the source of the cell lines BFTC-905 and T24 collected from a patient with bladder UC (grade III). These lines were subsequently cultured in RPMI-1640 medium. In addition, sodium pyruvate (1 mM), heat-inactivated fetal bovine serum (10%), and penicillin (100 U/mL)/streptomycin (100 µg/mL) were added to all culture media and the cells were cultured at 37°C with 5% CO_2.

Reagents and antibodies

Merck Millipore (Billerica, MA, USA) was the source of THZ1 and gemcitabine used in this study. CDK7, Bcl-2 (for western blotting), phospho-cdc2, phospho-histone H3, cleaved caspase-7, cleaved caspase-3, and cleaved PARP antibodies were purchased from Cell Signaling Technology (Danvers, MA, USA). Moreover, anti-β-actin and anti-glyceraldehyde-3-phosphate dehydrogenase (GAPDH) antibodies were sourced from GeneTex (Irvine, CA, USA), while anti-α-tubulin and anti-Bcl-2 [for immunohistochemistry (IHC)] antibodies were from Santa Cruz Biotechnology (Santa Cruz, CA, USA). The remaining chemicals used in our study were obtained from either Sigma-Aldrich (St. Louis, MO, USA) or Merck Millipore.

Cell viability

We assessed cell viability by performing the WST-1 assay (Biotools, Taipei, Taiwan). In brief, cells were seeded onto 96-well microplates (with a corresponding cell density of 5000 cells per well), after which they were subjected to incubation at 37°C for 24 h. The cells were then subjected to various treatments for the indicated periods of time, followed by incubation in WST-1-containing medium at 37°C for 4 h. A Multiskan™ GO plate reader (Thermo Fisher Scientific, Rockford, IL, USA) was employed to measure the absorbance of the resulting mixture at a measurement wavelength of 570 nm.

Western blotting

Lysis buffer (Cell Signaling Technology) in cold phosphate-buffered saline (PBS) was employed to lyse the cells, followed by a 10-min centrifugation process at 14000 rpm and 4°C. Subsequently, the amount of protein in the supernatant containing the cell lysate was measured using bicinchoninic acid protein assay (sourced from Thermo Scientific Pierce). Equal amounts of proteins from each group were mixed with loading buffer (Biotools) and then separated using sodium dodecyl sulfate-polyacrylamide gel electrophoresis. Following this, the separated proteins were transferred onto polyvinylidene fluoride membranes (Merck Millipore) and the membranes were blocked using bovine serum albumin (5%) in PBS. Subsequently, each of the membranes was incubated overnight with the indicated antibodies in PBS at 4°C. The membranes were then washed twice using TBS containing 0.05% Tween 20 (TBST), followed by a 2 h incubation process with horseradish peroxidase-conjugated secondary
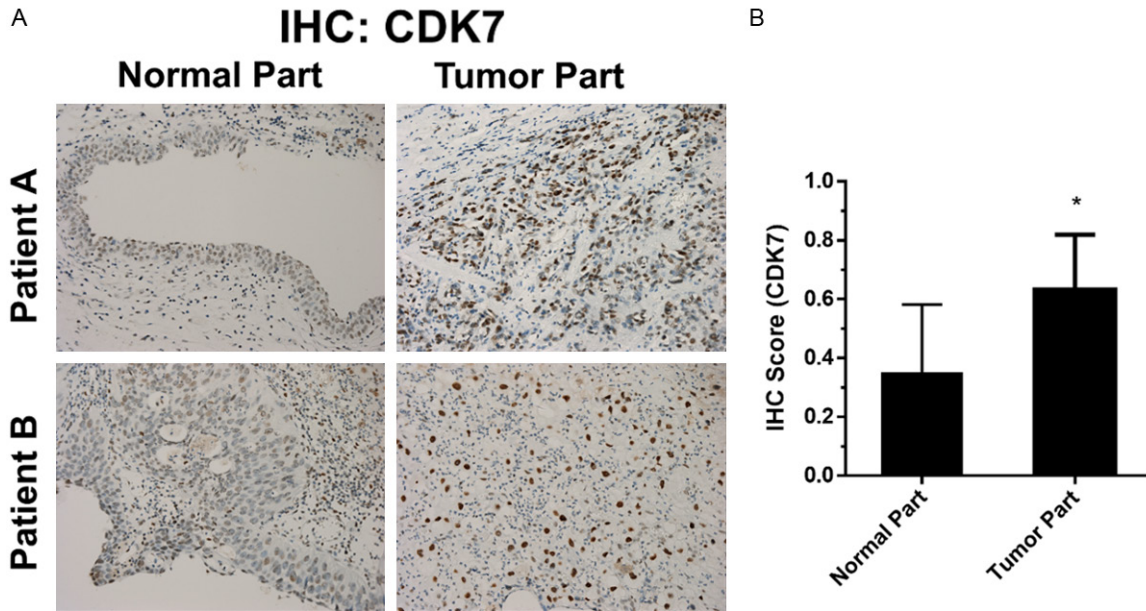
Figure 1. Assessment of CDK7 protein expression in UC samples using immunohistochemical staining. A. CDK7 expression in UC samples from 10 patients with muscle-invasive UC receiving radical cystectomy. Representative photographs of two samples showing expression of CDK7 in primary human UC sample, tumor versus normal urothelium. B. Quantitative IHC score measuring the immunoreactivity of CDK7, tumor versus normal urothelium. The data has been expressed as mean ± SD. *P<0.05 compared to normal urothelium group.

antibodies (GeneTex) at room temperature. Next, the antibody-labeled membranes were again washed twice with TBST. This was followed by imaging of the membranes on an ImageQuant LAS 4000 system (GE Healthcare) after treatment with enhanced chemiluminescence substrates (Merck Millipore and Biotools) [14].

Immunohistochemistry in human UC specimens

We included 12 patients with metastatic bladder who received systemic chemotherapy with the GC regimen. Of the 12 chemotherapy-treated patients, 6 experienced disease progression during chemotherapy and were categorized as 'chemo-resistant'; 6 showed response to chemotherapy and were categorized as 'chemo-sensitive'. We collected formalin-fixed paraffin-embedded tissue blocks from these individuals. The tissue blocks were cut into 5-µm-thick sections, after which IHC staining was performed on these sections using anti-Bcl-2 and anti-CDK7 antibodies, as described previously [14]. One of the authors (Lin W.C.), a board-certified pathologist specializing in urologic oncology, who was blinded to the clinical data, analyzed the IHC score based on the following criteria: staining intensity was divided into four categories, with 3 signifying strong, 2 moderate, 1 weak, and 0 negative staining. In addition, we evaluated the mean percentage of positivity by counting at least 10 random fields at 40× and 400× magnifications. The IHC score was calculated by multiplying the intensity score with the mean percentage of positivity. The current study was carried out according to the standard for the ethics of experimentation and research integrity. All experiments involving human participants were approved by the National Taiwan University College of Medicine Institutional Research Ethics Committee (No. 201412207RINA).

Cell proliferation assay

We evaluated the effect of THZ1 on UC cell proliferation using a commercial 5-bromo-2-deoxyuridine (BrdU) incorporation assay kit (Roche, Indianapolis, IN, USA). UC cells were seeded onto 96-well microplates at a density of 4000 cells per well. After 24 h, the cells were exposed to THZ1 or DMSO (control) for 48 h. Subsequently, the assay was carried out according to the protocol outlined by the manufacturer. The absorbance of each well was detected at the dual wavelengths of 450-540 nm using a Thermo Fisher Scientific Multiskan™ GO plate reader [14].
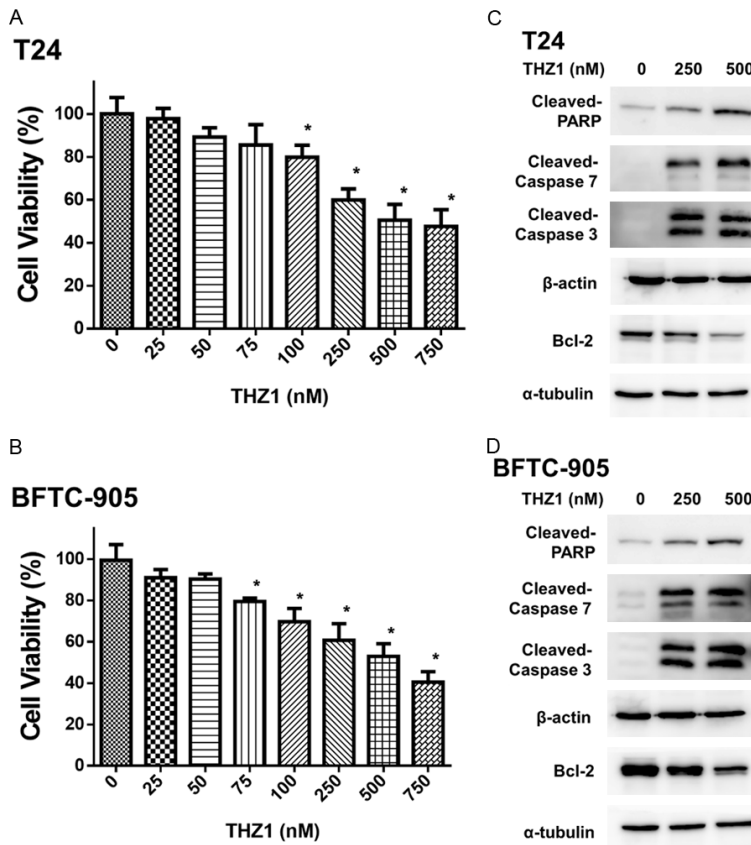
Figure 2. THZ1 induced cytotoxicity and apoptosis in human UC cells in a dose-dependent manner. (A) T24 and (B) BFTC-905 cells were treated for 24 h with various concentrations of THZ1 (0-750 nM) and DMSO (as control), respectively. Cell viability was assessed using WST-1 assay. The data have been presented as mean ± SD. *P<0.05 compared to control. (C) T24 and (D) BFTC-905 cells were exposed to THZ1 (250 and 500 nM) and DMSO (as untreated control) for 24 h, followed by harvesting of cell lysates. Western blot analyses show the level of cleaved-PARP, cleaved-caspase 7, cleaved-caspase 3, and Bcl-2. All results shown are representative of at least three independent experiments. Full-length blots are presented in Figure S1.

tumors were abscised and photographed. All the animal experiments reported herein were in accordance with the ARRIVE guidelines and were approved by the Institutional Animal Care and Use Committee (No. IACUC20170177) of the College of Medicine, National Taiwan University.

Statistical analysis

All the statistical analyses in this study were performed using Prism® 6 (GraphPad). The entirety of data was analyzed using one-way analysis of variance; the derived results have been presented herein as mean ± standard deviation. A p value of <0.05 was considered to signify statistical significance.

Results

CDK7 expression levels are higher in UC tumors than in the normal urothelium

The expression of CDK7 in UC was assessed by immunohistochemically staining tumors from ten clinical samples of radical cystectomy. The CDK7 immunoreactivity, along with the quantitative IHC score, was significantly higher in UC tumors than in normal urothelium counterparts (**Figure 1A**, **1B**).

THZ1 induces cytotoxicity and apoptosis in a dose-dependent manner in human UC cells

To investigate the antitumor effect of THZ1 on UC cells, we examined the viability of T24 and BFTC-905 cells after treatment for 24 h with 0-750 nM THZ1. Our results showed that THZ1 induced dose-dependent cytotoxicity in T24 and BFTC-905 cells (**Figure 2A**, **2B**). Additionally, we examined the apoptotic effect of THZ1 (250 and 500 nM) on T24 and BFTC-905 cells by measuring the cleavage of caspase-3, -7, PARP, and Bcl-2, an anti-apoptosis oncoprotein. THZ1 induced PARP, caspase-3, and caspase-7

In vivo xenograft model in nude mice

We suspended $5×10^5$ cells in serum-free media (100 µL) and then mixed them with an equivalent volume of Matrigel™ (BD Biosciences). Subsequently, the derived mixture was injected subcutaneously into the dorsal flanks of 8-week-old nude mice (Taiwan National Laboratory Animal Center, Taipei, Taiwan). After the tumor size reached 100-150-mm³, the mice received THZ1 (10 mg/kg/day), gemcitabine (10 mg/kg, administered twice per week), or gemcitabine plus THZ1 via intraperitoneal administration for 4 weeks. Tumor volume was measured every four days according to the formula: longest tumor diameter×(shortest tumor diameter)²/2. After the 4 week treatment, the
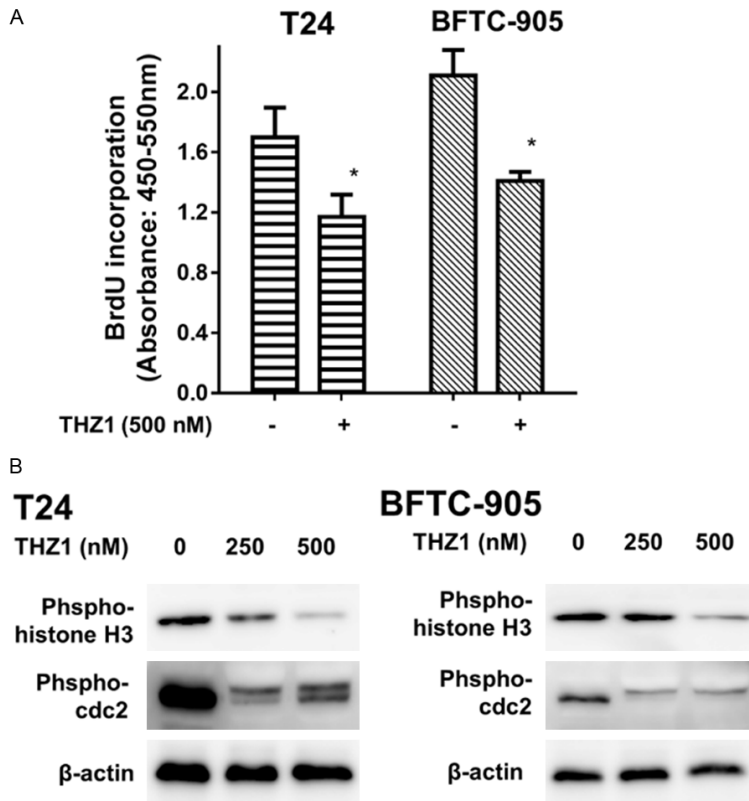
Figure 3. THZ1 inhibits cell proliferation and cell cycle transition in human UC cells. A. T24 and BFTC-905 cells were treated for 24 h with 500 nM THZ1 and DMSO (as control), respectively. BrdU assay was performed to estimate cell proliferation activity. The data have been presented as mean ± SD. *P<0.05 compared to control. B. Western blot was performed to evaluate the expression of cell cycle regulatory proteins, phospho-cdc2, and phospho-histone H3. Results shown are representative of at least three independent experiments. Full-length blots are presented in Figure S2.

arrest in cancer cells [15, 16]. Histone H3 is a nuclear core histone protein that regulates chromatin and functions in chromosome condensation and cell-cycle progression during the mitotic phase, after phosphorylation of the serine-10 residue. Our results indicated that THZ1 suppressed the expression of phospho-histone H3 (Ser 10) in UC cells.

THZ1 enhances gemcitabine-induced cytotoxicity via suppression of Bcl-2 in human UC cells

We then evaluated the cytotoxic effects of THZ1 in combination with cisplatin or gemcitabine on UC cells. The combined effects of TSA (0-500 mM) and gemcitabine (0-6 µM) on UC cells following exposure for 24 h were analyzed using WST-1 assay. THZ1 significantly enhanced gemcitabine-induced cytotoxicity (**Figure 4A**, **4B**). Western blot analysis of the expression of cleaved caspase-3, -7, and Bcl-2 showed that THZ1 suppressed gemcitabine-induced Bcl-2 overexpression and potentiated gemcitabine-related apoptosis (**Figure 4C**, **4D**). To further confirm the role of the Bcl-2 pathway in the combined effects of THZ1 and gemcitabine, we used ABT-199, a Bcl-2 inhibitor, and found that ABT-199 (10 µM) reduced cell viability to 74%, while co-treatment of THZ1 with ABT-199 did not significantly decrease the viability of the UC cells (**Figure 4E**, **4F**). Our results showed that THZ1 enhanced gemcitabine-induced cytotoxicity instead of cisplatin-induced cytotoxicity via suppression of Bcl-2.

cleavage with decreased Bcl-2 levels (**Figure 2C**, **2D**).

THZ1 inhibits cell proliferation and cell cycle transition in human UC cells

Furthermore, we examined the impact of THZ1 on cell proliferation and cell cycle transition in UC cells. Our results showed that there was a significant reduction in UC cell proliferation following exposure to 500 nM THZ1 for 24 h (**Figure 3A**). The phenomenon of THZ1-induced proliferation inhibition was accompanied by suppression of phospho-histone H3 (Ser 10) and phospho-CDC2 (**Figure 3B**). BrdU is commonly used for the detection of proliferating cells in living tissues because it gets incorporated into the newly synthesized DNA of replicating cells during the S phase. Previous studies have shown that THZ1 induces cell cycle

Bcl-2 overexpression is associated with chemotherapy resistance in patients with metastatic UCs

We then further compared the expression of Bcl-2 in UC tumors with chemo-sensitive and chemo-resistant status using IHC staining. As shown in **Figure 5A**, **5B**, the immunoreactivity
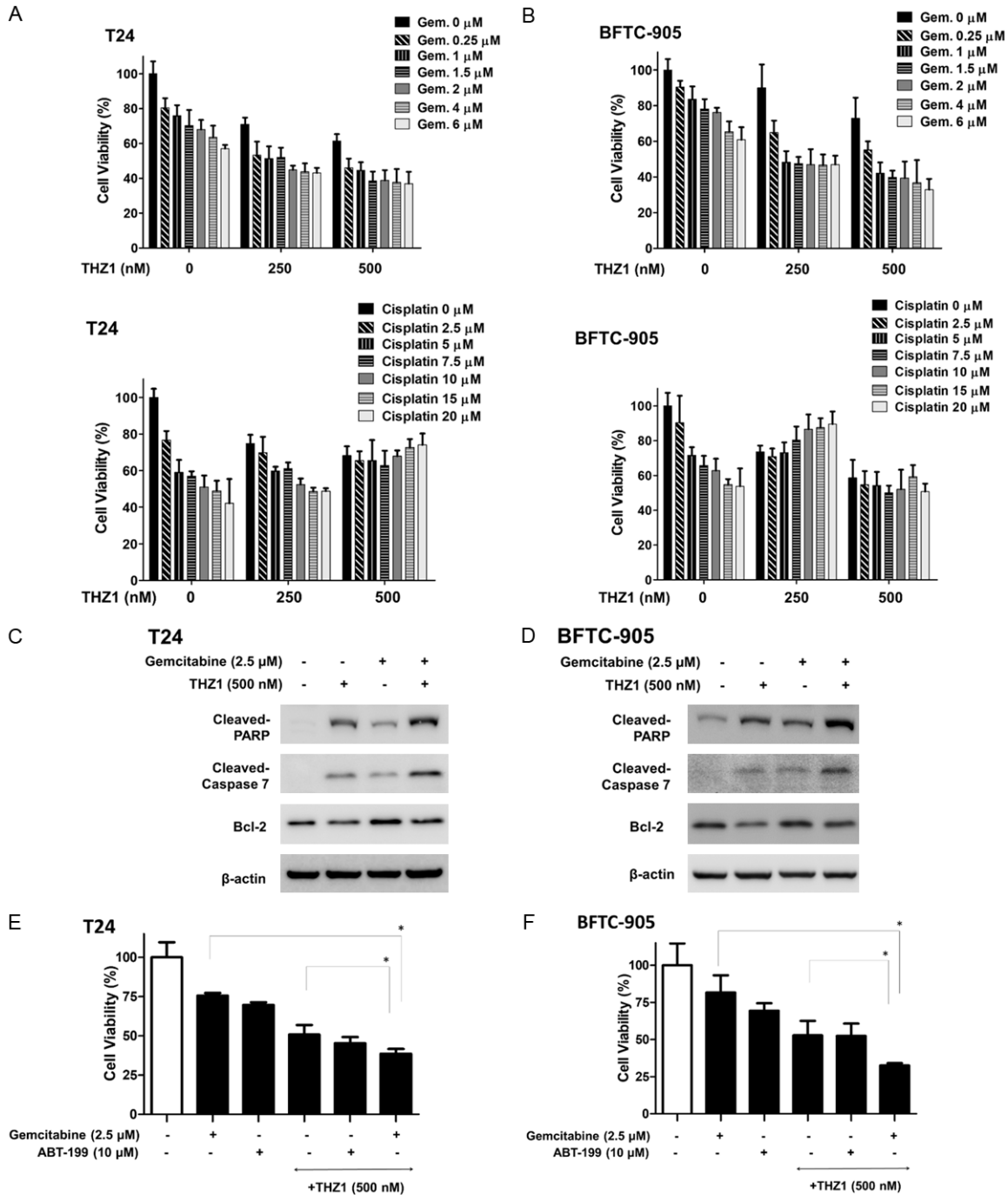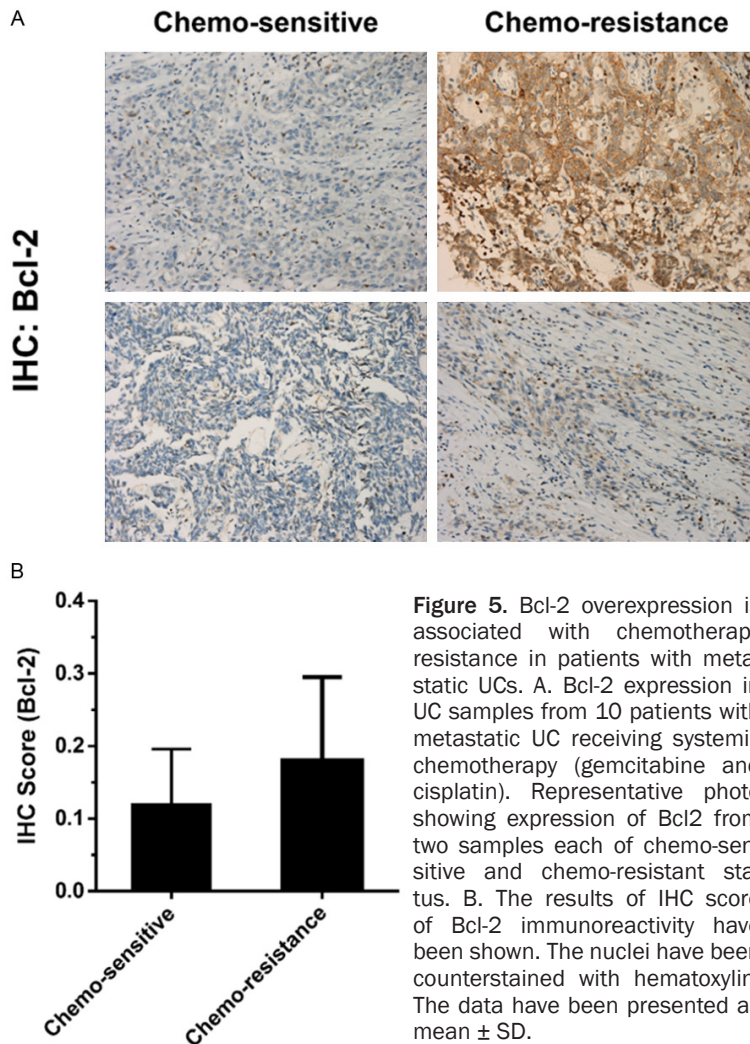
Figure 4. THZ1 enhances gemcitabine-induced cytotoxicity via suppression of Bcl-2 in human UC cells. (A) T24 and (B) BFTC-905 cells were treated with various concentrations of THZ1 (0, 250, and 500 nM) for 48 h in combination with various concentrations of gemcitabine (0-6 µM) and cisplatin (0-20 µM). Cell viability was assessed using WST-1 assay. (C and D) Western blot was performed to analyze the expression of cleaved-PARP, cleaved-caspase 7, and Bcl-2 after treatment with gemcitabine (2.5 µM) and THZ1 (500 nM) alone or in combination. (E) T24 and (F) BFTC-905 cells were treated with gemcitabine (2.5 µM), ABT-199 (10 µM), and THZ1 (500 nM) alone or in combination. Cell viability was measured using WST-1 assay. All data have been presented as mean ± SD of three independents experiments. Results are representative of at least three independent experiments. Full-length blots are presented in Figure S3.

of Bcl-2 was stronger in chemo-resistant UC tumors (lower part) than in chemo-sensitive tumors (upper part). These results demonstrat-

ed that Bcl-2 expression is associated with the sensitivity of chemotherapy in UC, consistent with previous results [17]. Bcl-2 overexpression

A

B

Figure 5. Bcl-2 overexpression is associated with chemotherapy resistance in patients with metastatic UCs. A. Bcl-2 expression in UC samples from 10 patients with metastatic UC receiving systemic chemotherapy (gemcitabine and cisplatin). Representative photo showing expression of Bcl2 from two samples each of chemo-sensitive and chemo-resistant status. B. The results of IHC score of Bcl-2 immunoreactivity have been shown. The nuclei have been counterstained with hematoxylin. The data have been presented as mean ± SD.

cer [19, 20]. The importance of CDK7 in cell cycle transition and transcription has highlighted CDK7 as a potential diagnostic and prognostic biomarker; moreover, it serves as a promising therapeutic target for cancer [12, 21]. Previous studies have reported that CDK7 is upregulated in various cancers and is associated with aggressive characteristics [22, 23]. In this study, we demonstrated distinctly higher expression of CDK7 in UCs than in counterpart urothelium. To the best of our knowledge, this is the first study to demonstrate an abnormal expression pattern of CDK7 in UCs.

Upregulation of CDK7 overexpression in human cancer makes it a remarkable therapeutic target for UC. THZ1, a covalent inhibitor of CDK7, elicits antitumor effects in various human tumors; however, its antitumor effect on bladder UC has never been reported. THZ1 inhibits phosphorylation of the C-terminal domain of RNAPII [24] and thus displays its effects via regulation of transcription. THZ1 also inhibits the activation of CDK proteins. It has been reported to disrupt the CDK7 signaling pathway. Since CDK7 is essential for the CDK-activating kinase activity, CDK7 inhibition by THZ1 causes transcription inhibition, cell cycle arrest, and cancer cell death [25]. Our results showed that THZ1 effectively induced antitumor effects, apoptosis, and cell cycle retardation in UC cells.

Additionally, cancer cells are characterized by decreased pro-apoptotic or increased anti-apoptotic signal molecules. A previous study indicated that cytotoxicity of THZ1 is mediated by reduced expression of anti-apoptotic proteins through inhibition of the STAT3 signaling pathway [26]. Bcl-2 is a member of the Bcl-2 family that regulates apoptosis by inhibiting anti-apoptotic factors or inducing pro-apoptotic factors [27]. Bcl-2 is important in the appropri-

is linked to chemoresistance in patients with metastatic UC [18].

THZ1 enhances gemcitabine-induced antitumor effects on UC xenograft in nude mice

We evaluated the antitumor effect of THZ1 in combination with gemcitabine in a xenograft nude mouse model. Temporal changes in tumor appearance and volume for each group during the 4-week treatment with saline/DMSO (sham control), THZ1 (10 mg/kg/day), gemcitabine (10 mg/kg, twice per week), or gemcitabine plus THZ1 via intraperitoneal administration are shown in **Figure 6A-D**. Consistently, THZ1 enhanced the antitumor effect of gemcitabine.

Discussion

Deregulation of the cell cycle and aberrant transcriptional control are common features of can-
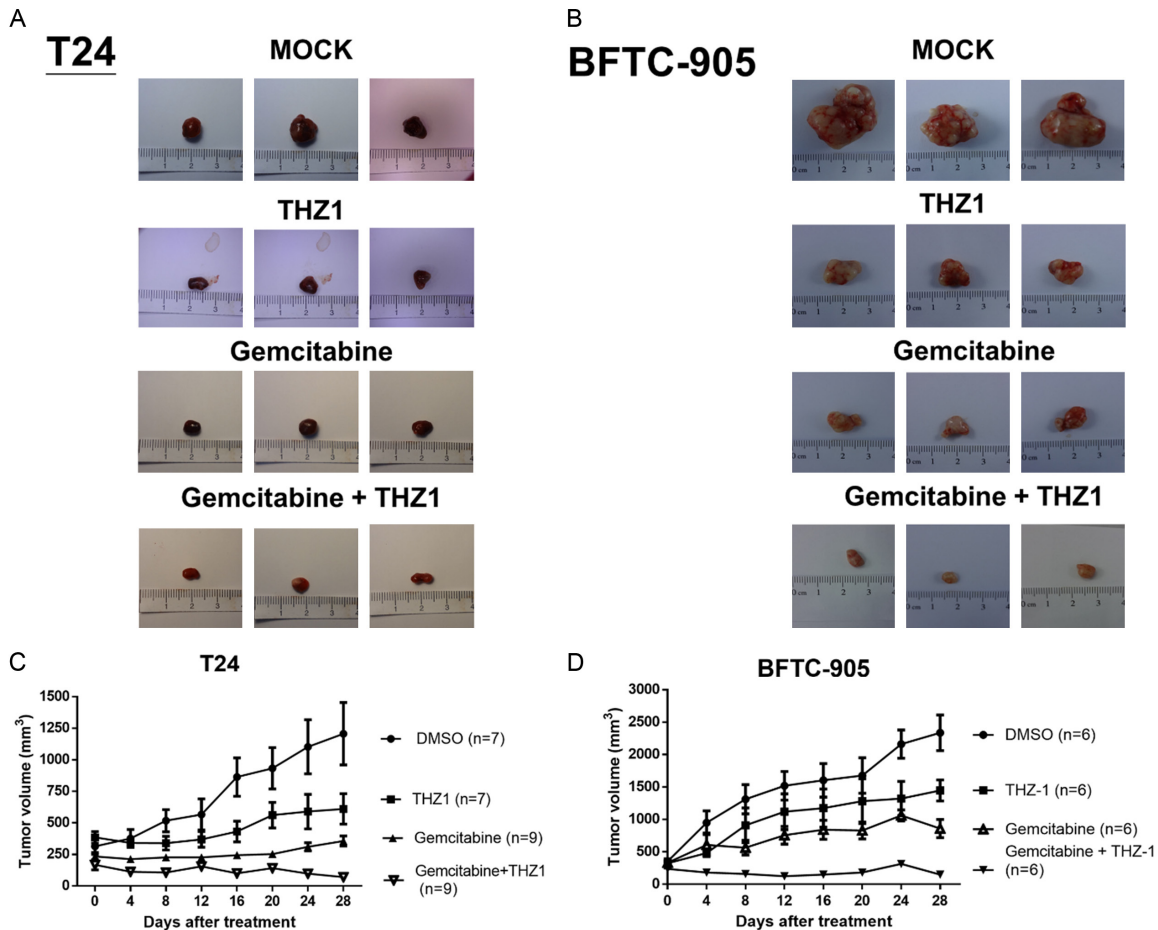
Figure 6. Xenograft nude mouse model demonstrates the efficacy of gemcitabine in combination with THZ1 *in vivo*. Nude mice bearing T24 or BFTC-905 xenograft tumors received intraperitoneal administration of saline/DMSO (as sham control, n=6), THZ1 (10 mg/kg/day, n=6), gemcitabine (10 mg/kg, twice per week, n=6), or a combination of gemcitabine and THZ1 (n=6) for 4 weeks. A and B show representative photos of T24 and BFTC-905 excised xenograft tumors from each group, respectively. C and D show T24 and BFTC-905 xenograft tumor volume (mm³) for each group, respectively, during the 4 week treatment. The data have been presented as mean ± SD. * P<0.05 represents a statistically significant difference between the cisplatin and combination groups.

ate operation of the apoptosis machinery [28]. Bcl-2 overexpression has been correlated with apoptosis evasion [29] and drug resistance [18]. Consistently, the results obtained in the present study upon IHC staining of clinical specimens demonstrated that Bcl-2 immunore-activity is associated with chemotherapy response. We further demonstrated that THZ1 suppressed Bcl-2 expression and augmented apoptosis in UC cells. Aberrant Bcl-2 expression and related chemotherapy resistance in UC cells provide a potential clinical application of targeting Bcl-2 to circumvent chemotherapy resistance.

The gemcitabine/cisplatin combination has become the most frequently adopted first-line treatment modality for metastatic bladder UC. However, the initial response rates are approximately 60% and the median survival with chemotherapy is approximately 12-18 months. Identifying novel drug combinations without overlapping toxicities and with improved efficacy has been an alternative strategy for UC treatment. In addition, the enriched feature patterns provide insights into the mechanisms underlying drug combinations. In this study, we investigated the antitumor efficacy of THZ1 in combination with gemcitabine or cisplatin. Our results demonstrated that THZ1 enhanced gemcitabine-induced cytotoxicity *in vitro* and *in vivo,* with concurrent suppression of gemcitabine-induced Bcl-2 activation. The drug combination improved the antitumor efficacy of

gemcitabine. The results of the present study provide a novel strategy for the treatment of metastatic UCs.

Conclusion

CDK7 may serve as a potential diagnostic biomarker for UC. The CDK7 inhibitor, THZ1, enhanced gemcitabine-induced cytotoxicity via suppression of Bcl-2. The aberrant expression of Bcl-2 after chemotherapy highlights Bcl-2 as a promising target to circumvent chemoresistance in human UC.

Acknowledgements

Disclosure of conflict of interest

None.

Address correspondence to: Kuo-How Huang, Department of Urology, National Taiwan University Hospital and National Taiwan University College of Medicine, Taipei, Taiwan. E-mail: khhuang123@ntu.edu.tw

References

[1] Siegel RL, Miller KD and Jemal A. Cancer statistics, 2015. CA Cancer J Clin 2015; 65: 5-29.

[2] Cohen MH and Rothmann M. Gemcitabine and cisplatin for advanced, metastatic bladder cancer. J Clin Oncol 2001; 19: 1229-1231.

[3] von der Maase H, Hansen SW, Roberts JT, Dogliotti L, Oliver T, Moore MJ, Bodrogi I, Albers P, Knuth A, Lippert CM, Kerbrat P, Sanchez Rovira P, Wersall P, Cleall SP, Roychowdhury DF, Tomlin I, Visseren-Grul CM and Conte PF. Gemcitabine and cisplatin versus methotrexate, vinblastine, doxorubicin, and cisplatin in advanced or metastatic bladder cancer: results of a large, randomized, multinational, multicenter, phase III study. J Clin Oncol 2000; 18: 3068-3077.

[4] von der Maase H, Sengelov L, Roberts JT, Ricci S, Dogliotti L, Oliver T, Moore MJ, Zimmermann A and Arning M. Long-term survival results of a randomized trial comparing gemcitabine plus cisplatin, with methotrexate, vinblastine, doxorubicin, plus cisplatin in patients with bladder cancer. J Clin Oncol 2005; 23: 4602-4608.

[5] Malumbres M. Physiological relevance of cell cycle kinases. Physiol Rev 2011; 91: 973-1007.

[6] Malumbres M and Barbacid M. Cell cycle, CDKs and cancer: a changing paradigm. Nat Rev Cancer 2009; 9: 153-166.

[7] Senderowicz AM. Targeting cell cycle and apoptosis for the treatment of human malignancies. Curr Opin Cell Biol 2004; 16: 670-678.

[8] Abate AA, Pentimalli F, Esposito L and Giordano A. ATP-noncompetitive CDK inhibitors for cancer therapy: an overview. Expert Opin Investig Drugs 2013; 22: 895-906.

[9] Jessen BA, Lee L, Koudriakova T, Haines M, Lundgren K, Price S, Nonomiya J, Lewis C and Stevens GJ. Peripheral white blood cell toxicity induced by broad spectrum cyclin-dependent kinase inhibitors. J Appl Toxicol 2007; 27: 133-142.

[10] Yin T, Lallena MJ, Kreklau EL, Fales KR, Carballares S, Torrres R, Wishart GN, Ajamie RT, Cronier DM, Iversen PW, Meier TI, Foreman RT, Zeckner D, Sissons SE, Halstead BW, Lin AB, Donoho GP, Qian Y, Li S, Wu S, Aggarwal A, Ye XS, Starling JJ, Gaynor RB, de Dios A and Du J. A novel CDK9 inhibitor shows potent antitumor efficacy in preclinical hematologic tumor models. Mol Cancer Ther 2014; 13: 1442-1456.

[11] Chipumuro E, Marco E, Christensen CL, Kwiatkowski N, Zhang T, Hatheway CM, Abraham BJ, Sharma B, Yeung C, Altabef A, Perez-Atayde A, Wong KK, Yuan GC, Gray NS, Young RA and George RE. CDK7 inhibition suppresses super-enhancer-linked oncogenic transcription in MYCN-driven cancer. Cell 2014; 159: 1126-1139.

[12] Christensen CL, Kwiatkowski N, Abraham BJ, Carretero J, Al-Shahrour F, Zhang T, Chipumuro E, Herter-Sprie GS, Akbay EA, Altabef A, Zhang J, Shimamura T, Capelletti M, Reibel JB, Cavanaugh JD, Gao P, Liu Y, Michaelsen SR, Poulsen HS, Aref AR, Barbie DA, Bradner JE, George RE, Gray NS, Young RA and Wong KK. Targeting transcriptional addictions in small cell lung cancer with a covalent CDK7 inhibitor. Cancer Cell 2014; 26: 909-922.

[13] Kwiatkowski N, Zhang T, Rahl PB, Abraham BJ, Reddy J, Ficarro SB, Dastur A, Amzallag A, Ramaswamy S, Tesar B, Jenkins CE, Hannett NM, McMillin D, Sanda T, Sim T, Kim ND, Look T, Mitsiades CS, Weng AP, Brown JR, Benes CH, Marto JA, Young RA and Gray NS. Targeting transcription regulation in cancer with a covalent CDK7 inhibitor. Nature 2014; 511: 616-620.

[14] Kuo KL, Ho IL, Shi CS, Wu JT, Lin WC, Tsai YC, Chang HC, Chou CT, Hsu CH, Hsieh JT, Chang SC, Pu YS and Huang KH. MLN4924, a novel protein neddylation inhibitor, suppresses proliferation and migration of human urothelial carcinoma: in vitro and in vivo studies. Cancer Lett 2015; 363: 127-136.

[15] Cheng ZJ, Miao DL, Su QY, Tang XL, Wang XL, Deng LB, Shi HD and Xin HB. THZ1 suppresses human non-small-cell lung cancer cells in vitro through interference with cancer metabolism. Acta Pharmacol Sin 2019; 40: 814-822.

[16] Zhang Y, Zhou L, Bandyopadhyay D, Sharma K, Allen AJ, Kmieciak M and Grant S. The covalent CDK7 inhibitor THZ1 potently induces apoptosis in multiple myeloma cells in vitro and in vivo. Clin Cancer Res 2019; 25: 6195-6205.

[17] Kuo KL, Liu SH, Lin WC, Chow PM, Chang YW, Yang SP, Shi CS, Hsu CH, Liao SM, Chang HC and Huang KH. The Deubiquitinating enzyme inhibitor PR-619 enhances the cytotoxicity of cisplatin via the suppression of anti-apoptotic Bcl-2 protein: in vitro and in vivo study. Cells 2019; 8: 1268.

[18] Sartorius UA and Krammer PH. Upregulation of Bcl-2 is involved in the mediation of chemotherapy resistance in human small cell lung cancer cell lines. Int J Cancer 2002; 97: 584-592.

[19] Hainaut P and Plymoth A. Targeting the hallmarks of cancer: towards a rational approach to next-generation cancer therapy. Curr Opin Oncol 2013; 25: 50-51.

[20] Hanahan D and Weinberg RA. Hallmarks of cancer: the next generation. Cell 2011; 144: 646-674.

[21] Jiang L, Huang R, Wu YP, Diao PF, Zhang W, Li J, Li ZW, Wang YL, Cheng J and Yang JR. Overexpression of CDK7 is associated with unfavourable prognosis in oral squamous cell carcinoma. Pathology 2019; 51: 74-80.

[22] Patel H, Abduljabbar R, Lai CF, Periyasamy M, Harrod A, Gemma C, Steel JH, Patel N, Busonero C, Jerjees D, Remenyi J, Smith S, Gomm JJ, Magnani L, Gyorffy B, Jones LJ, Fuller-Pace F, Shousha S, Buluwela L, Rakha EA, Ellis IO, Coombes RC and Ali S. Expression of CDK7, Cyclin H, and MAT1 is elevated in breast cancer and is prognostic in estrogen receptor-positive breast cancer. Clin Cancer Res 2016; 22: 5929-5938.

[23] Zhang ZF, Peng HX, Wang XJ, Yin X, Ma PF, Jing Y, Cai MC, Liu J, Zhang MY, Zhang SZ, Shi KX, Gao WQ, Di W and Zhuang GL. Preclinical efficacy and molecular mechanism of targeting CDK7-dependent transcriptional addiction in ovarian cancer. Mol Cancer Ther 2017; 16: 1739-1750.

[24] Ebmeier CC, Erickson B, Allen BL, Allen MA, Kim H, Fong N, Jacobsen JR, Liang K, Shilatifard A, Dowell RD, Old WM, Bentley DL and Taatjes DJ. Human TFIIH kinase CDK7 regulates transcription-associated chromatin modifications. Cell Rep 2017; 20: 1173-1186.

[25] Chow PM, Liu SH, Chang YW, Kuo KL, Lin WC and Huang KH. The covalent CDK7 inhibitor THZ1 enhances temsirolimus-induced cytotoxicity via autophagy suppression in human renal cell carcinoma. Cancer Lett 2020; 471: 27-37.

[26] Cayrol F, Praditsuktavorn P, Fernando TM, Kwiatkowski N, Marullo R, Calvo-Vidal MN, Phillip J, Pera B, Yang SN, Takpradit K, Roman L, Gaudiano M, Crescenzo R, Ruan J, Inghirami G, Zhang T, Cremaschi G, Gray NS and Cerchietti L. THZ1 targeting CDK7 suppresses STAT transcriptional activity and sensitizes T-cell lymphomas to BCL2 inhibitors. Nat Commun 2017; 8: 14290.

[27] Hardwick JM and Soane L. Multiple functions of BCL-2 family proteins. Cold Spring Harb Perspect Biol 2013; 5: a008722.

[28] Thomas S, Quinn BA, Das SK, Dash R, Emdad L, Dasgupta S, Wang XY, Dent P, Reed JC, Pellecchia M, Sarkar D and Fisher PB. Targeting the Bcl-2 family for cancer therapy. Expert Opin Ther Targets 2013; 17: 61-75.

[29] Reed JC. Bcl-2 on the brink of breakthroughs in cancer treatment. Cell Death Differ 2018; 25: 3-6.
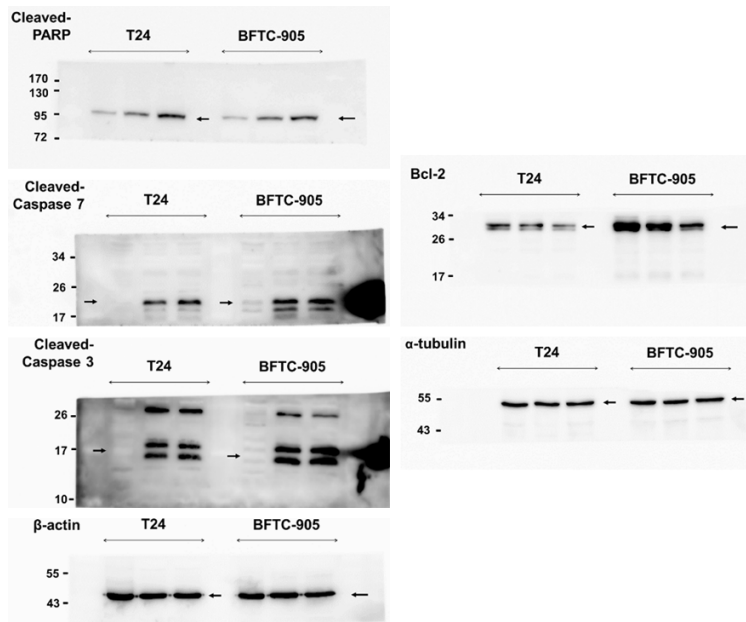
Figure S1. Full-length gels and blots corresponding to **Figure 2C**, **2D**. Molecular weight (kDa) has been shown in the left panel.
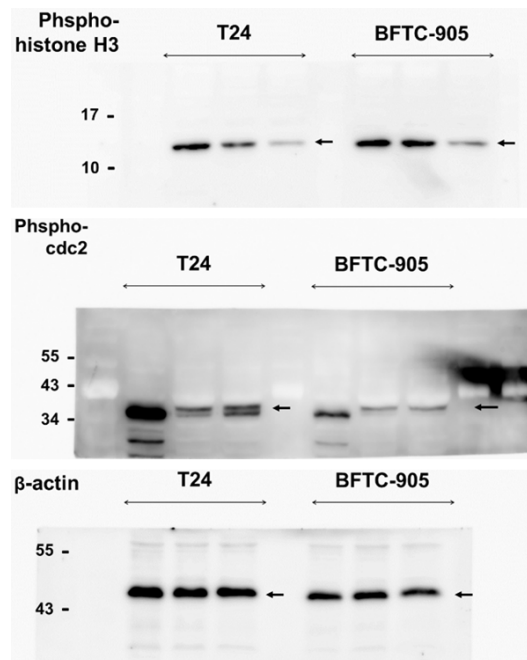

Figure S2. Full-length gels and blots corresponding to **Figure 3B**. Molecular weight (kDa) has been shown in the left panel.
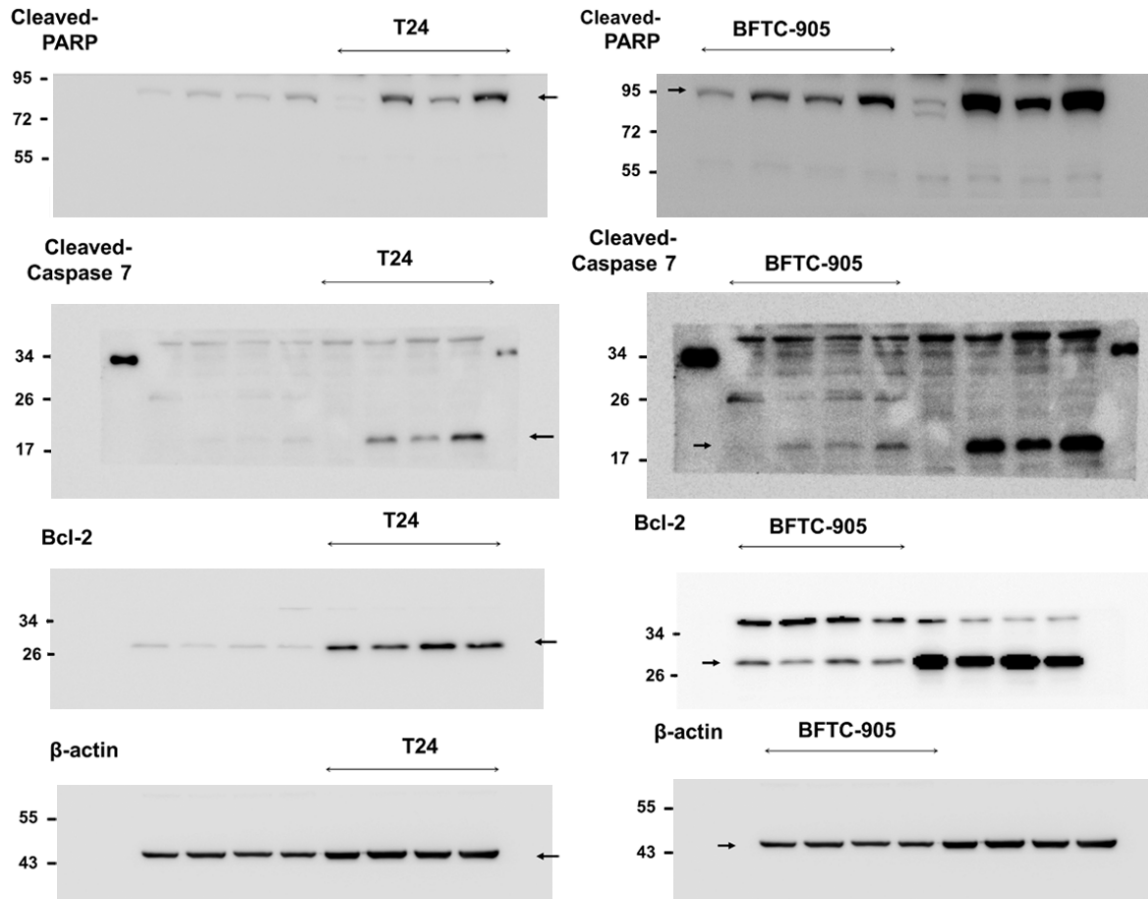
Figure S3. Full-length gels and blots corresponding to **Figure 4C**, **4D**. Molecular weight (kDa) has been shown in the left panel.